

# Glial cell missing-1 transcription factor is required for the differentiation of the human trophoblast

D Baczyk<sup>1,4</sup>, S Drewlo<sup>\*1,4</sup>, L Proctor<sup>1</sup>, C Dunk<sup>1</sup>, S Lye<sup>1,2</sup> and J Kingdom<sup>1,2,3</sup>

Mammalian placentation is a highly regulated process and is dependent on the proper development of specific trophoblast cell lineages. The two major types of trophoblast, villous and extravillous, show mitotic arrest during differentiation. In mice, the transcription factor, glial cell missing-1 (Gcm1), blocks mitosis and is required for syncytiotrophoblast formation and morphogenesis of the labyrinth, the murine equivalent of the villous placenta. The human homolog GCM1 has an analogous expression pattern, but its function is presently unknown. We studied GCM1 function in the human-derived BeWo choriocarcinoma cell line and in first trimester human placental villous and extravillous explants. The GCM1 expression was either inhibited by siRNA and antisense oligonucleotides methods or upregulated by forskolin treatment. Inhibition of GCM1 resulted in an increased rate of proliferation, but prevented *de novo* syncytiotrophoblast formation in syncytially denuded floating villous explants. GCM1 inhibition prevented extravillous differentiation along the invasive pathway in extravillous explants on matrigel. By contrast, forskolin-induced expression of GCM1 reduced the rate of proliferation and increased the rate of syncytialization in the floating villous explant model. Our studies show that GCM1 has a distinct role in the maintenance, development and turnover of the human trophoblast. Alterations in GCM1 expression or regulation may explain several aspects of two divergent severe placental insufficiency syndromes, namely preeclampsia and intrauterine growth restriction, which cause extreme preterm birth.

*Cell Death and Differentiation* (2009) 16, 719–727; doi:10.1038/cdd.2009.1; published online 13 February 2009

Successful mammalian pregnancy demands two key steps in placental development, both of which are regulated by differentiation of the epithelial trophoblast lineage.<sup>1</sup> First, maternal blood flow to the implantation site must increase exponentially to serve the demands of the rapidly growing fetus. This is achieved through the invasion of extravillous cytotrophoblasts (EV-CTs) from the base of the placenta into the maternal uterine stroma, where they surround and dilate the distal portions of the utero-placental arteries.<sup>2</sup> Second, the increased delivery of maternal blood to the placenta must be matched by an exchanger organ to transfer nutrients, remove waste products and respiratory gases between the mother and the developing fetus. This requirement is achieved through the expansion and differentiation of the chorionic villous trees of the placenta. These villi are covered by a villous trophoblast compartment comprising of villous cytotrophoblasts (V-CTs) beneath a continuous multinucleated layer of syncytiotrophoblast (SCT), which is in direct contact with maternal blood.<sup>3</sup>

In the human placenta, EV-CTs of the proximal portion of the anchoring villus cell column are proliferative, but more distal cells differentiate, as they invade and disperse into the uterine stroma. Here these cells surround and replace the smooth muscle cells of maternal uterine arteries, converting

them into high-flow dilated sinusoids. The arrest of EV-CT proliferation ensures that these cells do not invade too deeply into the myometrium and escape to other parts of the mother.

A similar phenomenon of cell-cycle arrest occurs in the human V-CT compartment. A subset of the V-CTs, residing on the basal lamina, enters the SCT by a process of syncytial fusion; the remaining V-CTs on the basal lamina continue to proliferate throughout pregnancy. The rate of syncytial fusion exceeds the amount that is required for villous growth; hence up to 3 g of V-CTs are shed as apoptotic material into the maternal circulation per day.<sup>4</sup>

In the most severe forms of human placental pathology resulting in fetal death, such as severe intrauterine growth restriction (IUGR), premature placental separation (abruption) and severe preeclampsia arising before 32 weeks of gestation, defects in both pathways of trophoblast development have been observed.<sup>5,6</sup> These defects include poor EV-CT invasion and transformation of the spiral arteries in severe early-onset preeclampsia,<sup>5,7</sup> and reduced elaboration of chorionic villous trees<sup>8,9</sup> with reduced numbers of proliferating V-CT in severe early-onset IUGR.<sup>10</sup> As arrest of mitosis is a common feature in both pathways of trophoblast differentiation (EV-CT and V-CT), we hypothesize that common defects

<sup>1</sup>Research Centre for Women's and Infants' Health (RCWIH) at the Samuel Lunenfeld Research Institute of Mount Sinai Hospital, University of Toronto, Toronto, Ontario, Canada; <sup>2</sup>Department of Obstetrics and Gynecology, Mount Sinai Hospital, University of Toronto, Toronto, Ontario, Canada and <sup>3</sup>Department of Pathology, Mount Sinai Hospital, University of Toronto, Toronto, Ontario, Canada

\*Corresponding author: S Drewlo, Samuel Lunenfeld Research Institute, Mount Sinai Hospital, 600 University Avenue, Toronto, Ontario, Canada M5G 1X5.

Tel: +1 416 586 4800 8322; Fax: +1 416 586 8565; E-mail: drewlo@mshri.on.ca

<sup>4</sup>These authors contributed equally to this work.

**Keywords:** glial cell missing-1; trophoblast; placental development; cytotrophoblast; proliferation; differentiation

**Abbreviations:** GCM1, Glial Cell Missing-1; EV-CT, Extravillous cytotrophoblast; V-CT, Villous cytotrophoblast; SCT, syncytiotrophoblast; IUGR, Intrauterine growth restriction; HELLP, Hemolysis Elevated Liver enzyme and Low Platelet count; hCG, Human chorionic gonadotropin; BrdU, bromodeoxyuridine; SDHA, Succinate dehydrogenase complex, subunit A; TBP, TATA box binding protein

Received 26.5.08; revised 05.12.08; accepted 19.12.08; Edited by RA Knight; published online 13.2.09

in cell-cycle regulation and trophoblast differentiation underlie these pathological conditions.

Cell-cycle arrest and labyrinthine trophoblast development in mice is regulated by the transcription factor, glial cell missing-1 (Gcm1).<sup>11</sup> Mouse embryos lacking Gcm1 die in mid-gestation because of a failure of SCT differentiation and, thus, lack of labyrinth formation – the murine equivalent of floating villous villi in the human placenta. In humans, the homolog GCM1 has an expression pattern similar to mice,<sup>12</sup> although its function in human trophoblast is presently not known. GCM1 is an upstream regulator of the fusion protein, Syncytin1, which is responsible for the fusion of cytotrophoblast into the overlying syncytium.<sup>13</sup> Both GCM1 and Syncytin1 are reduced in preeclampsia and HELLP (Hemolysis Elevated Liver enzymes and Low Platelet count) syndrome and may, therefore, be important contributors to this type of placental insufficiency.<sup>14,15</sup>

Understanding the molecular mechanisms that regulate human trophoblast proliferation and differentiation is key to our perception of severe placental pathologies of pregnancy. Using a human-derived BeWo choriocarcinoma cell line, and first trimester human villous and extravillous placental explant models, we show a central role for GCM1 in the regulation of key aspects of human placental development specifically with respect to (1) cytotrophoblast proliferation, (2) villous syncytial fusion and (3) extravillous trophoblast differentiation.

## Results

**GCM1 regulates the balance between cell–cell fusion and proliferation in BeWo cells.** The BeWo human choriocarcinoma cell line was used to assess GCM1-mediated syncytialization and proliferation. In these cells, fusion events were assessed with  $\beta$ -catenin immunofluorescence (Figure 1a–d) and fluorescence dual-color labeling for exact quantification purposes and to exclude cell division events (Supplementary Figure 1a–d). BeWo cells exhibit low spontaneous level of cell–cell fusion (Figure 1a), whereas forskolin treatment results in GCM1 induction through the cAMP pathway and stimulates cell–cell fusion (Figure 1b).<sup>16</sup> GCM1 silencing eliminated fusion in BeWo cells treated with forskolin (Figure 1c and d and Supplementary Figure 1c, d). The GCM1–siRNA interference in BeWo cells stably expressing siRNA resulted in  $90 \pm 5\%$  suppression of GCM1 mRNA levels (Figure 1e,  $P < 0.01$ ) and in  $42 \pm 13\%$  suppression of GCM1 protein levels (Figure 1f,  $P < 0.05$ ). Forskolin treatment significantly induced GCM1 mRNA level ( $>30$ -fold,  $P < 0.001$ ) and protein (1.5-fold,  $P < 0.05$ ) expression in non-silenced BeWo cells (cells treated with sense siRNA against GCM1) (Figure 1e and f,  $P < 0.05$ ). GCM1 protein levels in BeWo-treated cells were also monitored with immunocytochemistry (Supplementary Figure 2).

Fusion events were quantified using a two-color fusion assay by visualizing merging of the green and red dyes resulting from membrane dissolution (Supplementary Figure 1).<sup>17</sup> Forskolin-treated, non-silenced BeWo cells showed enhanced cell–cell fusion compared with non-silenced controls ( $13 \pm 0.08\%$  versus  $1.5 \pm 0.24\%$  fusion

events per number of nuclei,  $P < 0.01$ ) (Figure 1b and g and Supplementary Figure 1b). By contrast, GCM1 silencing in forskolin-treated BeWo cells resulted in reduced levels of cell–cell fusion compared with that in non-silenced forskolin-treated controls (Figure 1d and g and Supplementary Figure 1d). As the basal rate of cell–cell fusion in control BeWo cells was only 1.5%, we were unable to show further reduction in the fusion events in the GCM1–siRNA-treated BeWo cells (Figure 1g); however, we observed a four-fold reduction in secreted levels of hCG of the treated cells as compared with that of controls, suggesting that cell–cell fusion was inhibited (Supplementary Figure 1e).

BeWo cell proliferation was assessed over the 3-day culture period. By the third day of culture, forskolin-treated cells showed significantly reduced rate of proliferation as compared with controls ( $1.72 \times 10^5 \pm 1.08 \times 10^4$  versus  $2.46 \times 10^5 \pm 1.08 \times 10^4$  cells,  $P < 0.01$ ) (Figure 1h). Furthermore, GCM1 silencing resulted in a significantly increased proliferation rate in forskolin-treated cells compared with that in controls (Figure 1h).

Forskolin treatment resulted in a significant induction of cell–cell fusion and in a reduction of proliferation, whereas GCM1 silencing had the opposite effect. Non-silencing controls did not show a difference to non-treated BeWo cells in all experiments (data not shown).

Therefore, GCM1 expression levels display a direct positive correlation with fusion events (differentiation) and a negative correlation with proliferation.

## GCM1 is required for SCT differentiation in first trimester floating villous explants.

Untreated first trimester human placental explants display a distinctive single layer of V-CT (Figure 2a). Floating villous explants were selectively denuded of their SCT by enzymatic digestion, retaining a viable V-CT on the basal lamina, as described earlier (also shown in Figure 2b).<sup>18</sup> When left untreated, these explants spontaneously reformed their overlying SCT in the subsequent 48–72 h (Figure 2c). All experiments were carried out at 8% pO<sub>2</sub>, the physiological oxygen tension of first trimester explants.<sup>18</sup> The proliferative activity of these explants was assessed with Ki-67 immunohistochemistry (Figure 2d–f).

When explants were transfected with either siRNA or antisense oligonucleotides to GCM1 after denudation, we observed an inhibition of SCT reformation after 72 h (Figure 3a and d). Inhibition of GCM1 by either method resulted in the accumulation of  $4.9 \pm 1.5$  Ki67-positive layers of V-CTs, suggesting a promotion of cytotrophoblast proliferation at the expense of syncytial differentiation/fusion (Figure 3a and d; Table 1).

Parallel experiments using intact non-denuded villi, cultured with either antisense oligonucleotides (Figure 3b) or GCM1 siRNA (data not shown), showed a similar accumulation of Ki67-positive CT ( $3.8 \pm 0.4$  layers, Figure 3e; Table 1). Moreover, these explants displayed degenerating SCT with the dissolution of nuclei, suggesting necrosis and/or apoptosis (Figure 3b, arrowhead).

Forskolin-stimulated explants showed a thick SCT layer and reduced number of CT cell layers in comparison with controls ( $0.9 \pm 0.3$  versus  $2.1 \pm 0.3$  layer,  $P < 0.001$ ) and GCM1-silenced tissue (Figure 3c and f; Table 1).

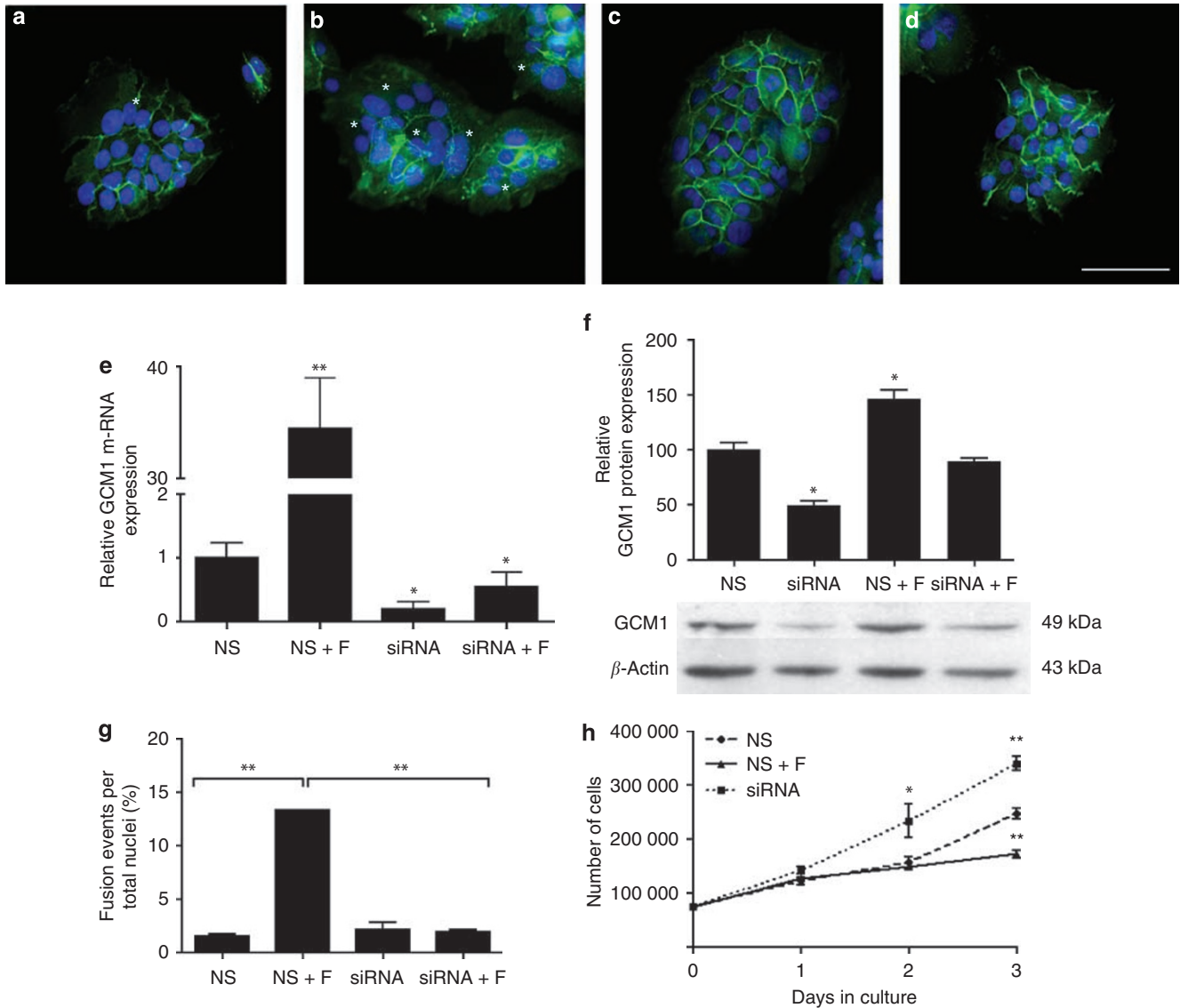


**Figure 1** Cell membrane integrity of BeWo cells was monitored with anti-human  $\beta$ -catenin immunofluorescence. (a) Immunofluorescent image of BeWo cells undergoing low spontaneous level of fusion (\* indicates 3 or more DAPI-stained nuclei within an intact membrane was considered as fusion event). (b) Forskolin-induced excessive cell-cell fusion resulted in membrane dissolution and loss of distinct membrane staining. (c) Silenced BeWo cells and (d) silenced BeWo cells treated with forskolin show no cell-cell fusion shown by intact membrane staining. Scale bar = 100  $\mu$ m. (e) Relative GCM1 mRNA expression ( $n=6$ ) and (f) representative western blot analysis of GCM1 protein expression ( $n=6$ ) in BeWo cells stably expressing siRNA to GCM1 in cells treated with 25  $\mu$ M of forskolin and in cells stably expressing siRNA + forskolin compared with non-silencing (sense control) siRNA-transfected control BeWo cells. Forskolin treatment of BeWo cells significantly upregulated GCM1 RNA and protein expression. GCM1 silencing eliminated this effect. Bar graph showing the mean  $\pm$  s.e. ( $n=6$ ). NS, non-silencing control; F, forskolin (25  $\mu$ M). (g) The two-color fusion assay shows a significant decrease of *de novo* fusion in the silenced BeWo group with forskolin treatment compared with that in control and forskolin-treated non-silenced BeWo cells. Difference between the non-forskolin-treated sense control group and stably expressing GCM1 siRNA group is not significant because of the low level of basal fusion ( $n=6$ ). (h) A proliferation assay of control BeWo cells, overexpressing GCM1 (25  $\mu$ M forskolin treatment) and BeWo cells stably expressing siRNA to GCM1 over 3 days in culture. On the third day of culture, cells overexpressing GCM1 show significant reduction in the number of cells, whereas BeWo cells stably expressing GCM1; siRNA show significant increase in cell numbers as compared with control cells ( $n=3$ ). Mock controls showed no difference to non-silenced controls in all experiments (data not shown). \* $P<0.005$ , \*\* $P<0.001$

These data indicate that GCM1 silencing of floating denuded explants promotes trophoblast proliferation at the expense of *de novo* SCT reformation. Forskolin-stimulated explants showed the opposite effect, resulting in an induction of GCM1 and a loss of cytotrophoblast cells owing to increased fusion events in the V-CT.

Western blot analysis of treated explants revealed significant reductions in GCM1 protein levels after siRNA ( $41 \pm 7.6\%$ ,

$P=0.002$ ) or antisense oligonucleotide ( $95 \pm 2.8\%$ ;  $P=0.001$ ) treatments, compared with control explants (Figure 3g).

Forskolin-stimulated explants resulted in GCM1 protein expression alterations in a time-dependent manner (Figure 3h). The GCM1 expression was significantly elevated during the first 5 h of treatment ( $31 \pm 11\%$   $P=0.03$ ) and declined after 18 h of cultivation. At 36 h, GCM1 level decreased by  $30 \pm 9\%$  ( $P=0.04$ ) most likely through the lack

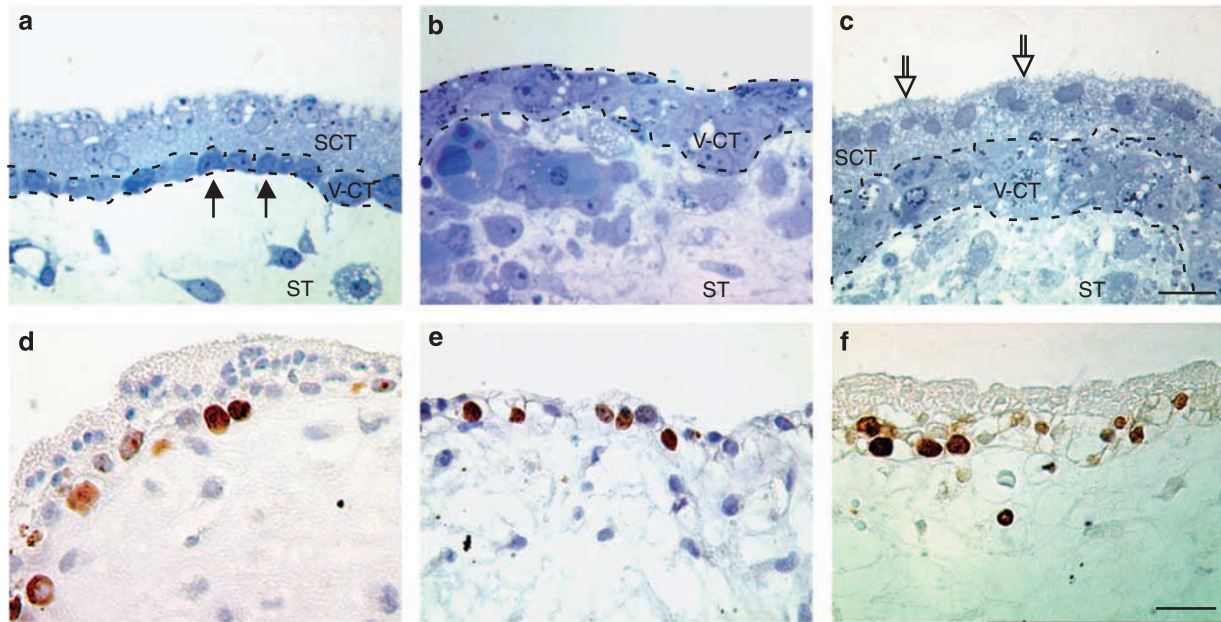


**Figure 2** Semi-thin toluidine blue-stained sections (a–c) and Ki-67-immunostained sections (d–f) of first trimester human placental explants cultured at 8% O<sub>2</sub>. (a) Representative image of untreated villous explant showing a distinctive single layer of cytotrophoblast cells (V-CT, ↑) and a healthy layer of overlying SCT. (b) Gentle trypsinization of explants and subsequent 24 h in culture results in a single-to-double layer of V-CT on the basal lamina and no overlying SCT. (c) Spontaneous regeneration of new SCT after 3 days in culture under control conditions (new syncytium ↓↓). Throughout the experiment, the explants retain proliferative activity as shown by Ki-67-positive staining; (d) T = 0, (e) post-trypsinization and (f) after 4 days in culture. Scale bars = 1000 μm (a–c); 50 μm (d–f). SCT, syncytiotrophoblast; V-CT, cytotrophoblast; ST, stroma

of proliferation and loss of GCM1-positive CT cells due to increased fusion events in these explants.

Proliferation events in our villous explant model were determined using bromodeoxyuridine (BrdU) incorporation. The relative proliferation index showed a significant six-fold increase in villous CT proliferation using antisense oligonucleotides ( $P=0.003$ ) and three-fold using siRNA against GCM1 compared with non-silenced controls. On the contrary, forskolin treatment reduced the BrdU index of proliferation by 40% ( $P=0.002$ ) (Figure 4).

Silencing of GCM1 expression through either siRNA or antisense oligonucleotide methods resulted in a significant increase in CT number and proliferation. Non-treated and vehicle-only control explants showed no significant difference compared with the non-silencing controls in all experiments (data not shown).

Together, semi-thin histology, proliferation index data and GCM1 western blot analysis results show that forskolin stimulation of floating villous explants initially induces an upregulation of GCM1 protein levels and syncytialization, but after 36–48 h of treatment, it leads to a depletion of proliferating cytotrophoblast cells due to an increased rate of fusion. On the other hand, our data indicate that the maintenance of normal SCT integrity requires continuous GCM1-initiated CT syncytial fusion events.

**GCM1 is required for extravillous trophoblast differentiation in first trimester explants.** First trimester explants plated onto Matrigel-coated cell inserts under hypoxic conditions (3%pO<sub>2</sub>) show the expansion of EV-CT number and migration of the EV-CT across and into the gel substrate (Figure 5a and b and Table 1).<sup>19,20</sup> The mean

number of outgrowth extensions in control oligonucleotide explants was  $7.5 \pm 3.1$  (Figure 5a). By contrast, explants cultured in media containing antisense oligonucleotide to GCM1 (Figure 5e and f) displayed a significant reduction in EV-CT invasion of the Matrigel ( $1.2 \pm 0.8$  outgrowths/explant;  $P < 0.001$ ). GCM1-silenced explants accumulated layers of CT at the point of contact with Matrigel (Figure 5f), and the accumulated cells were highly proliferative (data not shown). These accumulating cells were negative for the distal EV-CT marker,  $\alpha 1$ -Integrin (Figure 5g), thus indicating a proximal proliferative phenotype. In control explants, the distal outgrowths showed strong immunopositivity for  $\alpha 1$ -Integrin, suggesting differentiation to invasive EV-CT (Figure 5c). GCM1-silenced explants showed decreased immunopositivity of GCM1 (Figure 5h) in contrast to invading outgrowths under control conditions (Figure 5d). These data suggest that GCM1 promotes differentiation of the EV-CT, a process that involves a switch from proliferative to an invasive phenotype.

## Discussion

In this study, we show a central role for GCM1 in mediating the differentiation of trophoblast cells along both the villous and extravillous pathways in human placental development. Furthermore, we hypothesize that GCM1 regulates the important balance between proliferation and differentiation, a crucial step in the maintenance of the human placental function. Our conclusions are based on the results obtained using the human-derived choriocarcinoma cell line, BeWo, and first trimester human placental explants, cultured in conditions promoting either villous or EV-CT differentiation.

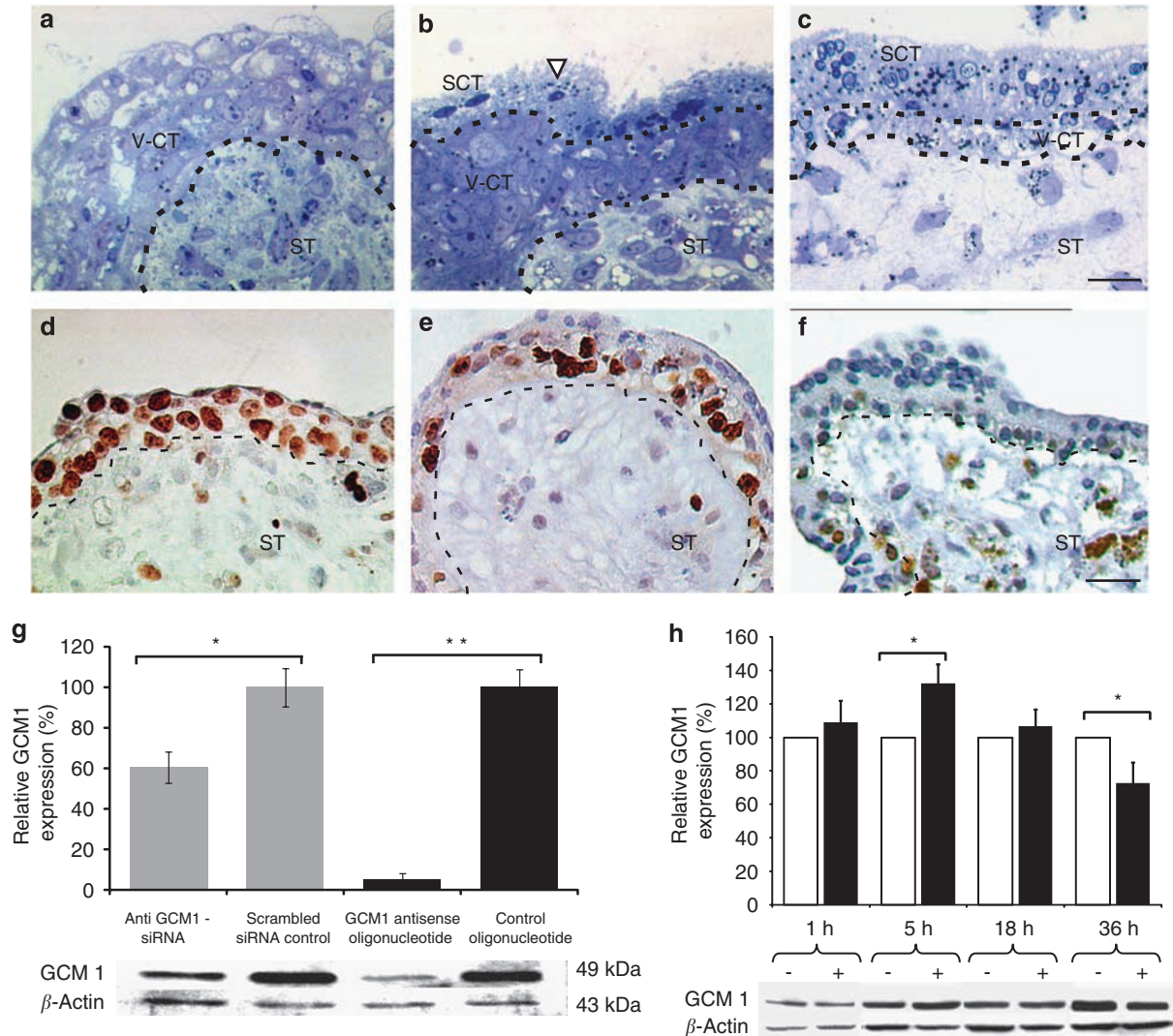


**Figure 3** GCM1 antisense oligonucleotides and siRNA treatment after trypsinization of SCT result in an accumulation of  $4.9 \pm 1.5$  layers of CT cells (semi-thin section, **a**) that proliferate (Ki-67 immunopositive in brown, **d**) but do not regenerate a new layer of SCT. (**b**) Treatment of non-denuded first trimester explants with GCM1 antisense oligonucleotide or siRNA results in the accumulation of  $3.8 \pm 0.4$  layers of cytotrophoblast cells underneath a necrotic SCT layer (note the dissolution of syncytial nuclei,  $\nabla$ ). (**e**) Accumulating V-CT exhibited a high level of proliferation (Ki-67 positive). (**c**) Forskolin treatment results in the accumulation of multilayer of syncytial nuclei, but reduced the numbers of V-CT cells ( $0.9 \pm 0.3$  layers) and (**f**) the rate of Ki-67 immunopositivity in the trophoblast layer. Scale bars =  $1000 \mu\text{m}$  (**a-c**),  $50 \mu\text{m}$  (**d-f**). (**g**) Western blot analysis of GCM1 protein levels in siRNA or antisense oligonucleotide-treated explants. (**h**) Forskolin treatment of first trimester floating villous explants regulates GCM1 protein levels in time-dependent manner. White bars = controls, black bars = forskolin-treated explants. Significant difference from control explants is indicated by  $*P < 0.05$

Our experiments show that alterations in GCM1 expression in human trophoblast induce changes in CT number, proliferation, SCT formation and EV-CT differentiation. In first trimester floating villous explants, reduced GCM1 expression results in an accumulation of proliferating CTs and degeneration of the overlying SCT due to the lack of syncytial fusion. GCM1 silencing in denuded villous explants prevents SCT regeneration. By contrast, the forskolin-induced upregulation of GCM1 expression has the opposite effect. In extravillous explants, the downregulation of GCM1 inhibits EV-CT formation. Therefore, we conclude that the regulation of GCM1 expression is critical for maintaining a balance between CT proliferation and differentiation in the first trimester.

GCM1 activity has been shown to be regulated at the post-translational level by acetylation, phosphorylation,<sup>21</sup> sumoylation and ubiquitination,<sup>22</sup> but its molecular regulation is still poorly understood. At the transcriptional level, GCM1 was shown to be regulated by a functional cAMP-responsive element and a histone deacetylase 3-binding motif in the promoter region upstream of the start codon.<sup>21,23,24</sup> GCM1 was shown to regulate the expression of different proteins, such as the placental growth factor,<sup>25</sup> a human aromatase,<sup>26</sup> and the fusion protein, Syncytin1.<sup>13</sup> A GCM1-binding motif was also found in the promoter of the human chorionic gonadotropin  $\alpha$ -subunit.<sup>26</sup> These findings support a complex and important role for GCM1 in placental maintenance and differentiation.

GCM1 is differentially expressed in cytotrophoblasts destined for syncytial fusion in both mice<sup>27</sup> and humans.<sup>12</sup> In our *in vitro* models, silencing of GCM1 expression in either the BeWo cell line or the first trimester villous explants resulted in the inhibition of cell–cell fusion, showing GCM1 role in the syncytialization process. This observation is consistent with the known effects of inhibiting syncytial fusion by blocking the activity of syncytin1, a direct downstream effector of GCM1.<sup>13</sup> Deficiency in syncytial fusion could have dramatic consequences on human pregnancy, as the SCT layer must be continuously regenerated to serve two important functions. First, the SCT must provide high levels of energy-dependent carrier systems that promote fetal

growth,<sup>28</sup> and second, SCTs express several anticoagulant proteins on their surface that prevent pathologic thrombosis of maternal blood perfusing the intervillous space.<sup>29</sup>

In human placenta, syncytial fusion involves initiating the early stages of the apoptosis cascade. Initiator caspases, such as caspase 8, are crucial for the differentiation and syncytial fusion of CT cells. Inhibition of the caspase 8 expression in human placental explants inhibits the progression of the apoptosis cascade and, thus, syncytial fusion.<sup>30</sup> Therefore, a controlled rate of apoptosis in the trophoblast layer is essential; imbalance in trophoblast turnover may lead to insufficient villi formation or degeneration of SCT.

Our experiments show that GCM1 also mediates *in vitro* EV-CT differentiation and trophoblast invasion, which is a key process in the *in vivo* transformation of the utero-placental spiral arteries. Under conditions that promote the invasive pathway of differentiation (extravillous explants of early first trimester villous tips in 3% oxygen), inhibition of GCM1 expression results in the accumulation of undifferentiated intermediate EV-CT.

We hypothesize that the morphologic consequences of GCM1 inhibition in floating villi, and in explanted villous tips invading Matrigel, are relevant to the development of important pathological disease states in pregnancy, especially the severe forms of preeclampsia and IUGR that cause birth before 32 weeks of pregnancy. In the severe form of preterm IUGR, the floating villi are small, underdeveloped<sup>8,9</sup> and show some evidence of reduced numbers of V-CT.<sup>10</sup> These observations suggest that in these pathologies, there may be a misbalance between cytotrophoblast proliferation and SCT formation. In the related disorder of severe early-onset preeclampsia, GCM1 is significantly downregulated.<sup>14</sup> Furthermore, immunohistochemical and morphometric analyses of preeclamptic placentae revealed an increase in proliferative activity of cytotrophoblast.<sup>31,32</sup> Therefore, these diseases might represent divergent end points resulting from

**Table 1** Number of cytotrophoblast layers in treated and control first trimester placental explants

	Number of CT layers in control explants	Number of CT layers in GCM1-silenced explants
Non-denuded floating explants	1.9 ± 0.4	3.8 ± 0.4*
Denuded explants	2.1 ± 0.3	4.9 ± 1.5*
	Number of CT layers in control explants	Number of CT layers in forskolin-treated explants
Non-denuded floating explants	1.9 ± 0.4	0.9 ± 0.3*
	Number of outgrowth fingers in control explants	Number of outgrowth fingers in GCM1-silenced explants
Matrigel explants	7.5 ± 3.1	1.2 ± 0.8*

\* $P < 0.001$ .

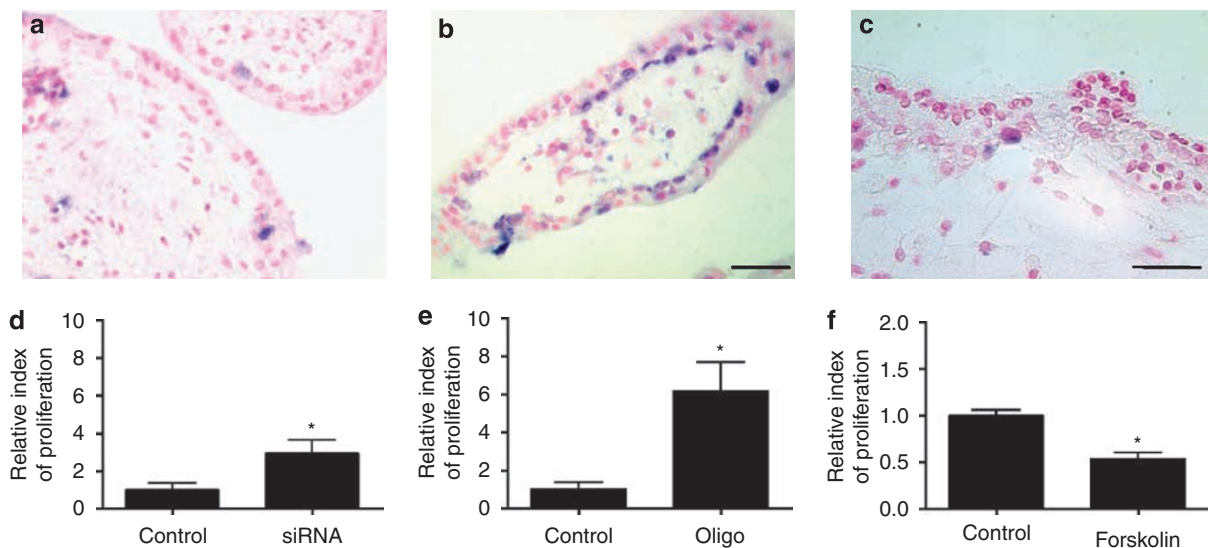


**Figure 4** Histological section of (a) control, (b) GCM1-silenced, and (c) forskolin-treated floating villous placental explants stained for BrdU (blue nuclei). The index of proliferation of villous trophoblast cells in explants cultured with (d) GCM1 siRNA, (e) the GCM1 antisense oligonucleotide and (f) forskolin. Scale bars = 40  $\mu\text{m}$  (a, b); 50  $\mu\text{m}$  (c).  $n = 9$ ; \* $P < 0.05$

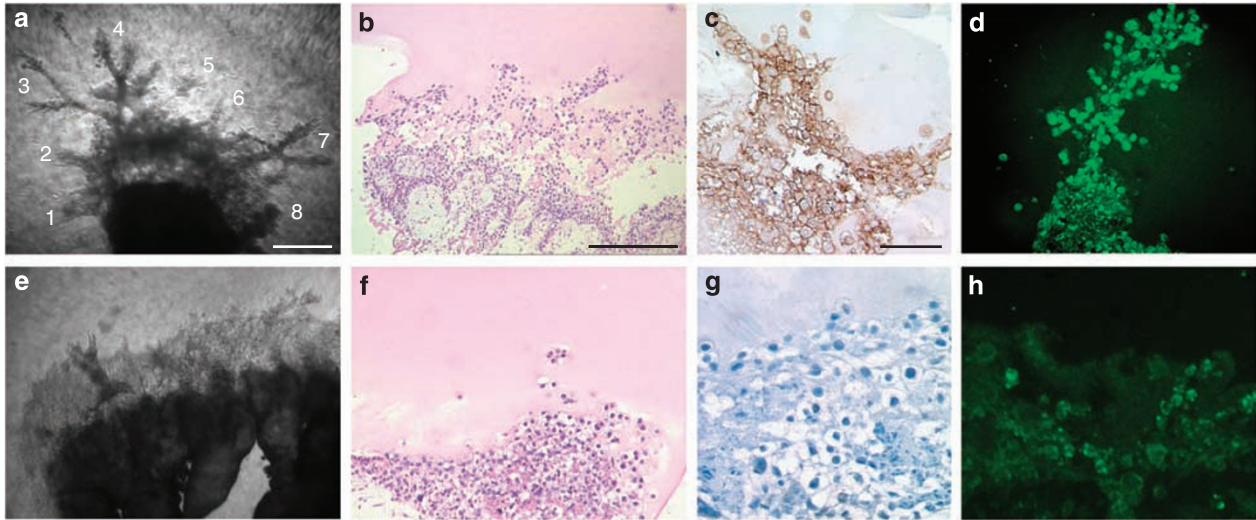


**Figure 5** Dissecting light microscope image of (a) sense oligonucleotide-treated first trimester explant cultured on Matrigel. Typical organized extravillous trophoblast outgrowth formation; eight outgrowth fingers are numbered. (b) H&E staining of control explants. (c) The outgrowths are  $\alpha 1$ -Integrin-positive as well as (d) GCM1-immunopositive. (e) GCM1 antisense oligonucleotide-treated explants do not form extravillous outgrowths, (f) cells do not invade Matrigel (H&E staining). (g) Cells are negative for the invasive marker  $\alpha 1$ -Integrin. (h) Immunofluorescent staining to GCM1 protein. Scale bars = 100  $\mu\text{m}$  (a, e); 50  $\mu\text{m}$  (b, f); 25  $\mu\text{m}$  (c, d, g, h)

**Table 2** Immunohistochemical reagents, probes and primers

Antigen	Antigen retrieval	Dilution	Reference
Ki-67	2 $\times$ 5 min <sup>a</sup>	1:100	DAKO (Carpinteria, CA, USA)
$\alpha 1$ -Integrin	Proteinase K	1:1500	Chemicon (Temecula, CA, USA)
BrdU	10% HCl (10 min)	1:10	Roche (Laval, QC, Canada)
$\beta$ -Catenin (6B3)	1 $\times$ 0.5 min <sup>a</sup>	1:50	Cell Signaling (Boston, MA, USA)
GCM1	2 $\times$ 5 min <sup>a</sup>	1:200	Kind gift from Dr H Chen (Taiwan)
GCM1 (western)		1:3000	Aviva System (San Diego, CA, USA)
$\beta$ -Actin (western)		1:2000	Sigma (Canada)
GCM1 primers	Forward: Reverse:	5'-ATGGCACCTCTAGCCCCTACA-3' 5'-GCTCTTCTTGCCCTCAGCTTCTAA-3'	
SDHA primers	Forward: Reverse:	5'-TGGGAACAAGAGGGCATCTG-3' 5'-CCACCACTGCATCAAATTCATG-3'	
TBP	—		Sequences are described in Bieche <i>et al</i> <sup>33</sup>

<sup>a</sup>High-temperature sodium citrate antigen retrieval pH 6.0. siRNA to GCM1 were designed to 5'-AACTCCGCGCATCCTCAAGAAG-3' and 5'-AACCTACAGTAGTGGAGACCT-3' DNA targets, named 201 and 815, respectively. NS control: 5'-TTCTCCGAACGTGTACAGT-3'. Stable shRNA were designed to 5'-AAGAAGTTAGAAGCCCTAGAA-3', 5'-AAGGGAGAGCATGATCATCCC-3' and 5'-AACCTACAGTAGTGGAGACCT-3' DNA targets named shRNA 1, 2, and 3, respectively. Sequence of Biognostik designed and manufactured antisense oligonucleotide to GCM1: 5'-AGAAGTTGGTGACCCG-3'.

pathological regulation of CT proliferation, syncytial differentiation, SCT shedding into maternal blood and EV-CT differentiation.

Understanding the mechanisms that govern CT cell survival in the human placenta, and the selective expression of GCM1 in CT destined for syncytial fusion or in EV-CT remodeling spiral arteries will improve our perception of the early origins of severe IUGR and preeclampsia caused by the so-called 'placental insufficiency.' Further studies of GCM1 regulation, together with an integration of stereologically determined villous trophoblast structure, are needed. The dual structural and molecular approach will effectively test the hypothesis that GCM1 regulation in CT is central to the origin of these important clinical diseases.

## Materials and Methods

**Retroviral gene transfer vector constructs.** We used the mammalian expression vector pSUPER-retro-puro (Oligoengine, Seattle, WA, USA) to direct intracellular synthesis of siRNA-like transcripts targeting GCM1 sequence. Three GCM1 shRNA DNA oligonucleotides and a non-silencing control were designed, annealed and ligated into the pSUPER-retro-puro vector (for sequence see Table 2).

**Retroviral transduction.** Phoenix amphotropic packaging cells (ATCC, Manassas, VA, USA) were transfected with the retroviral vectors (described above) using the BD CalPhos Mammalian Transfection Kit (BD Biosciences, Mississauga, ON, USA). Retroviral supernatants were collected, filtered and incubated with BeWo cells in the presence of 4  $\mu\text{g}/\text{ml}$  of cationic polymer-polybrene (Sigma, St Louis, MO, USA) to increase the efficiency of retrovirus-mediated gene transfer. After 48 h, cells transduced with GCM1 shRNA constructs were subjected to 2  $\mu\text{g}/\text{ml}$  puromycin (ICN Biomedicals, Irvine, CA, USA) selection for 7 days until all the

untransduced cells had died. The pools of resistant cells, 'stable transfectants,' were collected and processed for RT-PCR and western blot analysis to assess changes in the GCM1 mRNA and protein levels. Clone shiRNA-3 proved to be the most effective at silencing GCM1 levels and was thus used in the subsequent experiments.

**BeWo cell culture and fusion assay.** The human choriocarcinoma cell line BeWo (passages 10–20) and GCM1-silenced clone (shiRNA-3; passages 1–10) were maintained in F12K medium (ATCC) supplemented with 10% FBS, 100 units/ml penicillin, 100 units/ml streptomycin and 2.5  $\mu$ g/ml fungizone (Invitrogen, Burlington, ON, USA), in atmospheric O<sub>2</sub>/5% CO<sub>2</sub> at 37°C. Cell–cell fusion was assessed by two independent methods: anti-human  $\beta$ -catenin immunofluorescence staining was used to monitor the loss of cell membrane staining in fusing cells (Table 2, Figure 1a–d). Second, BeWo cells were color-labeled with Cell Tracker fluorescent dyes (Invitrogen) for analysis and quantification as described earlier.<sup>17</sup> Forskolin (final concentration 25  $\mu$ M) (Sigma, Oakville, ON, Canada) was added to accelerate syncytial fusion.<sup>18</sup> BeWo cells were assessed after 24 and 48 h for syncytial fusion using phase-contrast and fluorescent microscopy and quantified as described by Borges *et al.*<sup>17</sup> After 48 h, RNA was extracted from the cells using the RNeasy kit (Qiagen, Mississauga, ON, Canada), and protein was extracted using RIPA lysis buffer. For cell proliferation assay, 75 000 BeWo cells per well were plated into 24-well plates. Trypsinized cells were analyzed at 24, 48 and 72 h using the CASY TT cell counter (Innovatis, Hannover, Germany). All experiments were conducted in triplicate and replicated thrice for cell proliferation assay and six times for other experiments.

#### First trimester villous explant cultures

**Tissue collection.** First trimester placental villous tissues were collected from ultrasound-dated viable singleton pregnancies undergoing elective social termination of pregnancy between 6–12 weeks of gestation. Ethics committee approval was obtained from Mount Sinai Hospital Research Ethics board and all subjects gave written informed consent.

**Villous pathway.** Individual clusters of 8–12 week gestation villi were dissected in sterile cold PBS; the proximal stem villi were mounted under polystyrene cubes to float the villous trees in serum-free media (DMEM/F12) with 1% liquid media supplement ITS + 1 (Sigma, St Louis, MO, USA), 100 units/ml penicillin, 100 units/ml streptomycin, 2 mM L-glutamine, 100  $\mu$ g/ml gentamicin and 2.5  $\mu$ g/ml fungizone. These floating villous explants were cultured either with intact or enzymatically denuded SCT and maintained in 8% ambient oxygen (40 mm Hg) as recently described in detail.<sup>18</sup> A set of non-denuded explants was cultured with 25  $\mu$ M of forskolin (diluted in 100% ethanol). Explants were fixed and wax embedded to assess morphology at 0 h and throughout the duration of the experiments (24 and 48 h). Six random images of each experiment and treatment were assessed as follows: three random spots on the periphery of each villi per view were chosen to draw a perpendicular line to the stroma. Cells crossing this line were counted.

**Extravillous invasive pathway.** Individual clusters of 6–8 week villi were selected for the presence of EV-CT on villous tips. These clusters were explanted in Millicell-CM culture dish inserts (pore size 0.4  $\mu$ m, Millipore Corporation, Bedford, MA, USA) precoated with 200  $\mu$ l of phenol red-free Matrigel substrate (Becton Dickinson, Bedford, MA, USA). The explants were cultured in serum-free DMEM/F12 media supplemented with 100 units/ml penicillin, 100 units/ml streptomycin, 2 mM L-glutamine, 100  $\mu$ g/ml gentamicin and 2.5  $\mu$ g/ml fungizone, at 3% oxygen and 5% CO<sub>2</sub> as described earlier.<sup>19</sup> Explant tips were assessed for the initiation of column outgrowth formation at 24 h after establishment on Matrigel (success rate 90%). Only explants that showed successful initiation of outgrowth formation were used in the subsequent experiments. Throughout the experiments, outgrowths were monitored under a dissecting microscope by photography; the morphology of entire explants was documented at low power (Figure 5a and e;  $\times$  50) at the beginning of the experiment (24 h after establishment on Matrigel) and every 24 h thereafter. An 'outgrowth index,' defined as a total number of trophoblast fingers projecting from the periphery of the explant, was calculated and reported as mean  $\pm$  S.E. All explant experiments with cultured villi were conducted in triplicate and were replicated in four separate sets of explants.

**GCM1 siRNA, antisense oligonucleotide and forskolin treatment of explants.** Two double-stranded siRNA oligonucleotides (21mer) named 201 and 815 against the human GCM1 sequence were purchased from Qiagen (see sequences in Table 2). Phosphorothioate oligonucleotides and controls were

designed and manufactured by Biognostik (Gottingen, Germany) (sequence in Table 2). Floating villous and extravillous explants were incubated in the presence of either 1  $\mu$ M antisense oligonucleotides, sense oligonucleotides control, 100 nM siRNA or non-silencing siRNA control ( $n = 9$ ) (as described in Black *et al.*<sup>30</sup>). Non-treated controls showed no significant difference compared with the non-silencing control (data not shown). Experiments with fluorescent-labeled siRNA and antisense oligonucleotides established 80–90% transfection efficiency (data not shown). We exposed first trimester floating villous explants to 25  $\mu$ M forskolin and assessed CT proliferation and SCT differentiation.

All experiments were monitored for off-target effects with a human interferon- $\alpha$  ELISA kit (PBL Biomedical Laboratories) and toxicity was assessed using the LDH cytotoxicity Detection Kit (Sigma-Aldrich). Media from treated explants were analyzed and found negative for off-target effects and LDH activity (data not shown).

**Reverse transcription and real-time PCR.** Total RNA was extracted from BeWo cells or placental explants using the RNeasy kit (Qiagen). Dnase-treated RNA (1  $\mu$ g) was reverse-transcribed according to the manufacturer's instructions (Applied Biosystems Canada, Streetsville, ON, Canada). Samples were incubated at 25°C for 10 min, 42°C for 20 min and 95°C for 5 min. Real-time PCR was performed on an ABI Prism 7700 Sequence Detection System (ABI) in triplicates in 25  $\mu$ l volume containing 10 ng of template cDNA, 12.5  $\mu$ l of 2  $\times$  SYBR Green PCR Master Mix (ABI) and 50 nM of primers. GCM1 intron-spanning primers were designed using Primer Express 2.0 software (ABI) and sequences used are summarized in Table 2. The PCR program was initiated at 95°C for 10 min, followed by 40 thermal cycles of 15 s at 95°C and 60 s at 60°C. A melting curve for primer validation and a template standard curve were performed to show template-independent amplification results. The comparative C<sub>T</sub> method (ABI technical manual) was used to analyze the real-time PCR. The expression of GCM1 gene was normalized to the geometric mean of SDHA and TBP genes<sup>33</sup> and expressed as fold change relative to non-silenced (NS) controls ( $n = 7$ ).

**Western blotting for GCM1.** Total proteins were extracted from BeWo cells and placental explants as described earlier.<sup>18</sup> Protein lysates were assessed in 10% SDS-polyacrylamide gels and transferred on PVDF membranes (Millipore Corporation) (100 V constant for 1 h). Membranes were blocked with 5% skimmed milk in 0.1% (v/v) Tween Tris-buffer saline (TBST) for 2 h at room temperature and incubated with anti-GCM1 antibody (1:3000) at 4°C overnight (Aviva System Biology, San Diego, CA, USA). The membranes were washed with TBST and incubated with a secondary rabbit HRP-conjugated antibody for 1 h at room temperature. Antibody reaction was detected using the ECL detection kit (GE Health Care, Baie d'Urfe, QC, Canada). Data were standardized by stripping the blot and reprobing it with an anti- $\beta$ -actin antibody (Sigma-Aldrich). The results are presented as a ratio of relative optical density of the GCM1 band to the  $\beta$ -actin band and compared with the control samples ( $n = 6$ ).

**Histology and immunohistochemistry.** Paraformaldehyde-fixed placental explants were wax-embedded for hematoxylin and eosin (H&E) histology and immunohistochemistry. Entire floating villous and extravillous explants were serially sectioned and every fifth section was H&E stained to determine the three-dimensional structure of the explants. We confirmed that dissected floating villous explants did not contain preexisting columns and had a physiological monolayer of CT at the beginning of experiments; therefore, any subsequent accumulation of CT could be confirmed as a *de novo* event. Antibodies and antigen retrieval conditions are summarized in Table 2. Immunohistochemistry was performed on rehydrated sections with the streptavidin-biotin staining procedure, using Peroxidase Dako LSAB kit (Dako Canada Inc., Mississauga, ON, Canada) as described earlier.<sup>12</sup>  $\beta$ -Catenin immunofluorescence was performed on 3.7% formaldehyde fixed BeWo cells grown on coverslips. The slides were treated with 0.4% DAPI (4',6-diamidino-2-phenylindole) for nuclear detection. Fluorescence images were viewed using  $\times$  20 regular objective lens (NA 1.35) and collected using a DeltaVision Deconvolution microscope (Applied Precision, LLC, Issaquah, WA, USA).

Immunohistochemistry for BrdU (10  $\mu$ M) incorporation on floating villous placental explants<sup>34</sup> was performed according to the manufacturer's instruction. A proliferation index was calculated by dividing the number of BrdU-positive trophoblast nuclei by the total number of trophoblast nuclei counted in five adjacent fields of a 1 cm<sup>2</sup> graticule. Explants treated with antisense oligonucleotide, siRNA or forskolin were compared with control explants ( $n = 9$ ).



Negative controls included omission of the primary antibody and use of nonspecific matched IgG (Supplementary Figure 3). Slides were counterstained with hematoxylin (Sigma), visualized using a Nikon DMRX light microscope and photographed using a Sony PowerHAD 3CCD color video camera DXC-970MD (Sony, Toronto, ON, USA).

**Statistical analysis.** Data are presented as mean with errors expressed in S.E. Unpaired *t*-tests and the Mann–Whitney rank-sum tests were used to test for significance between treatment and the non-silenced controls in normal and non-normal data, if not otherwise stated. One-way ANOVA and the Tukey's *post hoc* test were used to compare the proportion of fusion events in BeWo cells between multiple treatment groups. BeWo cell proliferation was analyzed by two-way ANOVA with treatment and duration in culture as factors, followed by Tukey's *post hoc* test. To analyze forskolin-treated explants, two-way ANOVA, time and treatment as fixed effects, has been used. Data were normalized within culture relative to the negative treatment. There was a significant interaction between positive and negative treatment ( $P < 0.050$ ), and Bonferroni's *post hoc* test was carried out to compare the effect of treatment at each time point. All statistical calculations were performed using SigmaStat<sup>®</sup> 3.1 software and *P*-values  $\leq 0.05$  were considered significant.

**Acknowledgements.** The authors thank Dr. Oksana Shynlova for critical reading of the manuscript, Niki Radulovich for help with retroviral infections, as well as the donors and the BioBank Program of the CIHR Group in Development and Fetal Health (CIHR no. MGC-13299), the Samuel Lunenfeld Research Institute and the MSH/UHN Department of Obstetrics and Gynecology for the human specimens used in this study. Anti-GCM1 antibody for immunohistochemistry was a kind gift from Dr. H Chen (Taiwan). This study was supported by the Physician's Services Inc. Ontario (Grant no. 01-44) and the Canadian Institutes of Health Research (Grant no. 64302) to JK.

- Cross JC. Formation of the placenta and extraembryonic membranes. *Ann N Y Acad Sci* 1998; **857**: 23–32.
- Robson SC, Simpson H, Ball E, Lyall F, Bulmer JN. Punch biopsy of the human placental bed. *Am J Obstet Gynecol* 2002; **187**: 1349–1355.
- Benirschke K, Kaufmann P. *Pathology of the Human Placenta*, 4th edn, Springer-Verlag: New York, 2006.
- Huppertz B, Frank HG, Kingdom JC, Reister F, Kaufmann P. Villous cytotrophoblast regulation of the syncytial apoptotic cascade in the human placenta. *Histochem Cell Biol* 1998; **110**: 495–508.
- Viero S, Chaddha V, Alkazaleh F, Simchen MJ, Malik A, Kelly E *et al*. Prognostic value of placental ultrasound in pregnancies complicated by absent end-diastolic flow velocity in the umbilical arteries. *Placenta* 2004; **25**: 735–741.
- Toal M, Keating S, Machin G, Dodd J, Adamson SL, Windrim RC *et al*. Determinants of adverse perinatal outcome in high-risk women with abnormal uterine artery Doppler images. *Am J Obstet Gynecol* 2008; **198**: 330; e331–e337.
- Reister F, Frank HG, Kingdom JC, Heyl W, Kaufmann P, Rath W *et al*. Macrophage-induced apoptosis limits endovascular trophoblast invasion in the uterine wall of preeclamptic women. *Lab Invest* 2001; **81**: 1143–1152.
- Jackson MR, Walsh AJ, Morrow RJ, Mullen JB, Lye SJ, Ritchie JW. Reduced placental villous tree elaboration in small-for-gestational-age pregnancies: relationship with umbilical artery Doppler waveforms. *Am J Obstet Gynecol* 1995; **172** (2 Part 1): 518–525.
- Krebs C, Macara LM, Leiser R, Bowman AW, Greer IA, Kingdom JC. Intrauterine growth restriction with absent end-diastolic flow velocity in the umbilical artery is associated with maldevelopment of the placental terminal villous tree. *Am J Obstet Gynecol* 1996; **175**: 1534–1542.
- Macara L, Kingdom JC, Kaufmann P, Kohnen G, Hair J, More IA *et al*. Structural analysis of placental terminal villi from growth-restricted pregnancies with abnormal umbilical artery Doppler waveforms. *Placenta* 1996; **17**: 37–48.
- Anson-Cartwright L, Dawson K, Holmyard D, Fisher SJ, Lazzarini RA, Cross JC. The glial cells missing-1 protein is essential for branching morphogenesis in the chorioallantoic placenta. *Nat Genet* 2000; **25**: 311–314.
- Baczyk D, Satkunaratnam A, Nait-Oumesmar B, Huppertz B, Cross JC, Kingdom JC. Complex patterns of GCM1 mRNA and protein in villous and extravillous trophoblast cells of the human placenta. *Placenta* 2004; **25**: 553–559.
- Yu C, Shen K, Lin M, Chen P, Lin C, Chang GD *et al*. GCMa regulates the syncytin-mediated trophoblastic fusion. *J Biol Chem* 2002; **277**: 50062–50068.
- Chen CP, Chen CY, Yang YC, Su TH, Chen H. Decreased placental GCM1 (glial cells missing) gene expression in pre-eclampsia. *Placenta* 2004; **25**: 413–421.
- Knerr I, Beinder E, Rascher W. Syncytin, a novel human endogenous retroviral gene in human placenta: evidence for its dysregulation in preeclampsia and HELLP syndrome. *Am J Obstet Gynecol* 2002; **186**: 210–213.
- Wice B, Menton D, Geuze H, Schwartz AL. Modulators of cyclic AMP metabolism induce syncytiotrophoblast formation *in vitro*. *Exp Cell Res* 1990; **186**: 306–316.
- Borges M, Bose P, Frank HG, Kaufmann P, Potgens AJ. A two-colour fluorescence assay for the measurement of syncytial fusion between trophoblast-derived cell lines. *Placenta* 2003; **24**: 959–964.
- Baczyk D, Dunk C, Huppertz B, Maxwell C, Reister F, Giannoulas D *et al*. Bi-potential behaviour of cytotrophoblasts in first trimester chorionic villi. *Placenta* 2006; **27**: 367–374.
- Huppertz B, Kingdom J, Caniggia I, Desoye G, Black S, Korr H *et al*. Hypoxia favours necrotic versus apoptotic shedding of placental syncytiotrophoblast into the maternal circulation. *Placenta* 2003; **24**: 181–190.
- Genbacev O, Zhou Y, Ludlow JW, Fisher SJ. Regulation of human placental development by oxygen tension. *Science* 1997; **277**: 1669–1672.
- Chang CW, Chuang HC, Yu C, Yao TP, Chen H. Stimulation of GCMa transcriptional activity by cyclic AMP/protein kinase A signaling is attributed to CBP-mediated acetylation of GCMa. *Mol Cell Biol* 2005; **25**: 8401–8414.
- Chou CC, Chang C, Liu JH, Chen LF, Hsiao CD, Chen H. Small ubiquitin-like modifier modification regulates the DNA binding activity of glial cell missing *Drosophila* homolog a. *J Biol Chem* 2007; **282**: 27239–27249.
- Chuang HC, Chang CW, Chang GD, Yao TP, Chen H. Histone deacetylase 3 binds to and regulates the GCMa transcription factor. *Nucleic Acids Res* 2006; **34**: 1459–1469.
- Knerr I, Schubert SW, Wich C, Amann K, Aigner T, Vogler T *et al*. Stimulation of GCMa and syncytin via cAMP mediated PKA signaling in human trophoblastic cells under normoxic and hypoxic conditions. *FEBS Lett* 2005; **579**: 3991–3998.
- Chang M, Mukherjee D, Gobble RM, Groesch KA, Torry RJ, Torry DS. Glial cell missing 1 regulates placental growth factor (PGF) gene transcription in human trophoblast. *Biol Reprod* 2008; **78**: 841–851.
- Yamada K, Ogawa H, Honda S, Harada N, Okazaki T. A GCM motif protein is involved in placenta-specific expression of human aromatase gene. *J Biol Chem* 1999; **274**: 32279–32286.
- Cross JC, Nakano H, Natale DR, Simmons DG, Watson ED. Branching morphogenesis during development of placental villi. *Differentiation* 2006; **74**: 393–401.
- Sibley CP, Birdsey TJ, Brownbill P, Clarson LH, Doughty I, Glazier JD *et al*. Mechanisms of maternofetal exchange across the human placenta. *Biochem Soc Trans* 1998; **26**: 86–91.
- Krikun G, Lockwood CJ, Wu XX, Zhou XD, Guller S, Calandri C *et al*. The expression of the placental anticoagulant protein, annexin V, by villous trophoblasts: immunolocalization and *in vitro* regulation. *Placenta* 1994; **15**: 601–612.
- Black S, Kadyrov M, Kaufmann P, Ugele B, Emans N, Huppertz B. Syncytial fusion of human trophoblast depends on caspase 8. *Cell Death Differ* 2004; **11**: 90–98.
- Arnholdt H, Meisel F, Fandrey K, Lohrs U. Proliferation of villous trophoblast of the human placenta in normal and abnormal pregnancies. *Virchows Arch* 1991; **60**: 365–372.
- Brown LM, Lacey HA, Baker PN, Crocker IP. E-cadherin in the assessment of aberrant placental cytotrophoblast turnover in pregnancies complicated by pre-eclampsia. *Histochem Cell Biol* 2005; **124**: 499–506.
- Bieche I, Laurendeau I, Tozlu S, Olivivi M, Vidaud D, Lidereau R *et al*. Quantitation of MYC gene expression in sporadic breast tumors with a real-time reverse transcription-PCR assay. *Cancer Res* 1999; **59**: 2759–2765.
- Lavillette D, Maurice M, Roche C, Russell SJ, Sitbon M, Cosset FL. A proline-rich motif downstream of the receptor binding domain modulates conformation and fusogenicity of murine retroviral envelopes. *J Virol* 1998; **72**: 9955–9965.

Supplementary Information accompanies the paper on Cell Death and Differentiation website (<http://www.nature.com/cdd>)